Anomalous surface diffusion of water compared to aprotic liquids in nanopores

J.-P. Korb,[1,*] M. Whaley Hodges,[2] Th. Gobron,[1] and R. G. Bryant[2]
[1]*Laboratoire de Physique de la Matière Condensée, CNRS, Ecole Polytechnique, 91128 Palaiseau, France*
[2]*Department of Chemistry, University of Virginia, Charlottesville, Virginia 22901*
(Received 15 January 1999)

^{1}H nuclear magnetic relaxation dispersion experiments show remarkable differences between water and acetone in contact with microporous glass surfaces containing trace paramagnetic impurities. Analyzed with surface relaxation theory on a model porous system, the data obtained for water show that proton surface diffusion limited by chemical exchange with the bulk phase permits long-range effectively one-dimensional exploration along the pores. This magnetic-field dependence coupled with the anomalous temperature dependence of the relaxation rates permits a direct interpretation in terms of the proton translational diffusion coefficient at the surface of the pores. A universal rescaling applied to these data collected for different pore sizes and on a large variety of frequencies and temperatures, supports this interpretation. The analysis demonstrates that acetone diffuses more slowly, which increases the apparent confinement and results in a two-dimensional model for the molecular dynamics close to surface relaxation sinks. Surface-enhanced water proton diffusion, however, permits the proton to explore a greater spatial extent of the pore, which results in an apparent one-dimensional model for the diffusive motions of the water that dominate nuclear spin relaxation. [S1063-651X(99)04209-9]

PACS number(s): 68.45.Kg, 68.35.Fx, 76.60.Es

I. INTRODUCTION

Liquid dynamics at solid surfaces is central to understanding transport properties in heterogeneous systems such as rocks, catalytic materials, or biological tissues. Characterization of liquids at surfaces is difficult because the small fraction of liquid in a surface layer is generally in rapid exchange with bulk phases in contact with it. Nuclear magnetic relaxation dispersion (MRD), the measurement of nuclear spin-lattice relaxation rates as a function of magnetic field strength or nuclear Larmor frequency, provides a powerful approach for characterizing molecular dynamics, including surface dynamics, because the relaxation is directly related to correlation functions for the fluctuating magnetic interactions that depend on intra and intermolecular dynamics. Thus, models for molecular motions may be tested directly [1–4].

Here we report remarkable differences in the ^{1}H MRD between water and other common aprotic solvents such as acetone when in contact with high-surface-area calibrated microporous chromatographic glasses that contain trace paramagnetic impurities located at or close to the pore surface. Moreover the temperature dependences of the ^{1}H MRD of water and aprotic solvents are opposite. Although the calibrated glass does not provide a one-dimensional matrix, the molecular dynamics of water ^{1}H spin relaxation is dominated by long-range correlations that make the dynamics appear one-dimensional. On the other hand, when probed with the larger acetone molecule, the dynamics appears to be two-dimensional. In spite of the low paramagnetic concentration, a common observation is that the spatial confinement of aprotic liquids diffusing in close proximity to a surface causes a bilogarithmic dependence of the proton (I) spin-lattice relaxation rate, $1/T_1$, on Larmor frequency [4]. The $\frac{10}{3}$ slope ratio that we observed in these bilogarithmic dispersion curves is an unambiguous signature of a spin relaxation dominated by paramagnetic relaxation centers (S) [4]. The diamagnetic contributions are at least an order of magnitude smaller than paramagnetic ones because the nuclear-spin relaxation rate is proportional to the square of the product of the magnetogyric ratios for the electron γ_S, and proton γ_I, with $\gamma_S = 658.21\gamma_I$ [5]. Further, the spin-relaxation rate is enhanced because of the numerous re-encounters between I and S spins induced by the confinement [4].

Water is unique in that it is small, has extensive hydrogen bonding capabilities, and may exchange protons with other molecules or surface sites. It may behave as both a Lewis acid or base, and generally coordinates to most metal ions. The water proton spin-lattice relaxation rate is fundamentally different from that of other liquids studied on glasses to date in that it shows a power-law dependence on magnetic field strength. We demonstrate that this dependence results from I-S correlations that persist much longer in the surface region than in the bulk, thus leading to a significant increase of $1/T_1$. We also show that the nuclear spin-lattice relaxation rate at the pore surface is dominated by dynamic processes that appear to be one-dimensional. An interesting feature is that the temperature dependence is opposite to that usually observed for diffusion-induced relaxation, which is found for aprotic liquids. We may interpret the anomalous temperature dependence in terms of a diffusive process at the pore surface, which is interrupted by a chemical exchange with the bulk phase. The fundamental difference between water and other solvents in these glasses is the spatial extent of the surface explored by the diffusing protons of the liquid. The possibility that water may coordinate directly to paramagnetic relaxation centers is shown to be of minor importance to the observed relaxation dispersion profiles.

*Author to whom correspondence should be addressed.

TABLE I. Porous glass characteristics.

Measured characteristics	Sample $S1$	Sample $S2$
Pore radius R (Å)	39.5	79.5
Paramagnetic iron content (ppm)	45[a]	36[a]
Pore volume: V_p (cc/g)	0.47	0.81
Specific area: S_p (m^2/g)	140	91
Pore distribution	6%	5.8%
Mass glass: m_g (g)	0.67	0.43
Mass water: m_w (g)	0.92	1.14
Glass density: ρ (g/cm^3)	2.4	2.4

[a]Measured by chemical analysis and electron paramagnetic resonance spectroscopy.

II. NUCLEAR MAGNETIC RELAXATION DISPERSION OF WATER IN CONFINEMENT

A. Samples

Controlled pore chromatographic glasses were obtained from the Sigma Company with mean pore diameters of 75 and 159 Å and a specific area of $S_p = 140\,m^2/g$ and 91 m^2/g, respectively. Sample characteristics are listed in Table I. The water used was obtained from a Barnstead nanopure deionizer that included a carbon filter and used deionized water as a source. Samples were prepared gravimetrically by depositing a known mass of glass beads in a 10-mm pyrex glass sample tube, fitted with a screw cap, filled with water, and shaken vigorously. The glass beads were permitted to settle for several hours, excess water removed by pipet, and the total mass recorded. Sample tubes were finally doubly sealed with rubber stoppers and a screw cap.

The iron content of these samples, monitored by chemical analysis and electron-paramagnetic-resonance (EPR) spectroscopy, was 45 and 36 ppm for the 75 and 159 Å pore glasses labeled in the following as $(S1)$ and $(S2)$, substitute for the Si or Al in the glass matrix. Were there iron that dissolved in the aqueous phase, the ^{1}H MRD would be characteristic and fundamentally different from that observed [6,7]. Let us suppose that our glass sample is composed of a closed-packed set of spheres of SiO_2. From the specific area, $S_p = 140\,m^2/g$, density $\rho = 2.4\,g/cm^2$, and intersilicon separation $\Delta r = 3.6$ Å, one may compute that the proportion of Si tetraedra at the surface of these small spheres $S_p \rho \Delta r = 0.12$ for $S1$ and 0.08 for $S2$. The radii r_s of these spheres may be found by comparison of such a proportion to the ratio of volumes $(4\pi r_s^2 \Delta r / 4\pi r_s^3/3) = 0.12$, giving $r_s = 94$ Å (for $S1$) and 144 Å (for $S2$). The iron atoms in the first layer of the pore surfaces are unique because they may have open coordination positions that may bind the H_2O directly. The remaining iron atoms are deeper in the glass. The electron-nuclear dipolar interaction depends on $1/r_{IS}^6$ where r_{IS} is the proton (I)-electron (S) distance, so that the paramagnetic ions buried below the pore surface are much less effective in relaxing mobile protons in the liquid. Assuming a homogeneous spherical distribution of an Fe atom in the glass, one has an average distance, $\langle d_{\text{Fe-H}} \rangle = \langle 1/r_{IS}^6 \rangle^{-1/6} \sim (\frac{5}{3} r_{IS}^5 r_S)^{1/6} = 5.3$ Å for $S1$ and 5.7 Å for $S2$, between a given Fe in the glass and a proton at surface, which is about the distance of the 2nd layer from the surface. From this distribution, one has a proportion: $\{1 - [(r_S - \langle d_{\text{Fe-H}} \rangle)/r_s]^3\} \sim 0.16$ for $S1$ and ~ 0.12 for $S2$, of Fe atoms located at a distance $\langle d_{\text{Fe-H}} \rangle$ from the surface. The surface density σ_S of paramagnetic centers S is thus $45 \times 10^{-6} (N_{\text{Avogadro}}/55.85)/S_p 0.16 = 5.53 \times 10^{10}\,\text{Fe}\,\text{cm}^{-2}$ for the $S1$ and $5.1 \times 10^{10}\,\text{Fe}\,\text{cm}^{-2}$ for $S2$. The average distance between the paramagnetic centers located at distance $\langle d_{\text{Fe-H}} \rangle$ from the pore surface is then of the order of $1/\sqrt{\sigma_S} = 432$ Å for $S1$ and 442 Å for $S2$, i.e., much larger than the pore diameters.

B. Experiments

Proton nuclear magnetic relaxation rates were measured using a field cycling instrument of the Redfield design and constructed with S. Koenig and R. Brown as described elsewhere [8–10]. The ^{1}H magnetic relaxation dispersion profiles for aqueous suspensions in $S1$ and $S2$ chromatographic glass beads are reported in Figs. 1(a) and 1(b) for magnetic fields corresponding to ^{1}H Larmor frequencies ν_I from 0.01 to 30 MHz and a range of temperatures from 5 to 45 °C. Basically, one observes a strong dependence on magnetic field strength at low fields and an asymptotic plateau at large fields. We will show in the following that such a plateau is characteristic to a relaxation process driven by fast molecular motions. Moreover, the temperature dependence is different at low and at high magnetic field strengths for $S1$ [Fig. 2(a)] and $S2$ [Fig. 2(b)]. At low magnetic fields, the increase in the proton relaxation rate with increasing temperature is consistent with a chemical exchange process (Fig. 2). At large fields, the decrease in the observed rates with increasing temperature is characteristic of relaxation driven by a bulk diffusion process (Fig. 2). In order to isolate the frequency-dependent term of the overall proton relaxation rate, we have subtracted, for each temperature, the respective high-field asymptotic constant values from the data in Figs. 1(a) and 1(b). This procedure results in the relaxation dispersion curves shown in Figs. 1(c) and 1(d). The dependence that we observe, $1/T_1(\nu_I) \propto 1/\sqrt{\nu_I}$, persists for more than three orders of magnitude in the magnetic field strength. We will show in the following that this power law and its anomalous temperature dependence, shown in Fig. 2 at low magnetic fields, may result from enhanced diffusive motion at the pore surface that is interrupted by a chemical exchange with the bulk phase. The situation is very different for an aprotic solvent such as acetone, which is larger and has no labile or exchangeable protons. Here one observes a bilogarithmic frequency dependence for the ^{1}H acetone MRD in both $S1$ and $S2$ [Figs. 3(a) and 3(b)]. An interesting feature is that the temperature dependence is opposite to that for water. We have shown that these MRD are consistent with a theory that treats the mobile protons from the viewpoint of a two-dimensional restricted diffusion in close proximity to the relaxing surface centers [4]. The fundamental difference from the water case is the size of the effective diffusion constant and the spatial extent of the surface explored by the diffusing protons.

III. THEORY OF HETERONUCLEAR DIPOLAR RELAXATION BY TRANSLATIONAL DIFFUSION OF WATER IN NANOPORES

A. Biphasic fast exchange model

We apply the basic principles of spin relaxation in liquids caused by sparsely distributed electronic spins at the pore

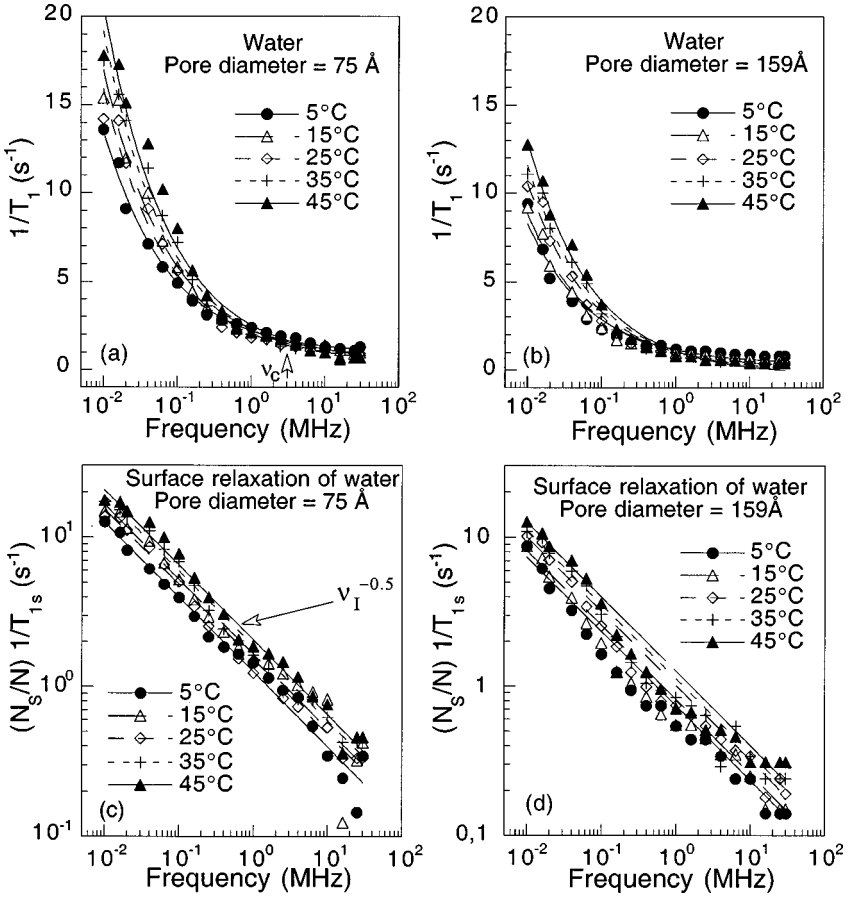

FIG. 1. The water ^{1}H spin-lattice relaxation rates as a function of magnetic field strength represented as the Larmor frequency for packed samples of calibrated porous glass beads with pore diameters 75 Å (a) and 159 Å (b) at various temperatures. The continuous lines correspond to the best fits to Eqs. (3) and (18) as discussed in the text. (c) and (d) Logarithmic plots of the dispersion curves obtained from Figs. 1(a) and 1(b) by subtracting the corresponding asymptotic high field values [see Eq. (4)]. The continuous lines correspond to the best fits obtained with Eq. (18).

surface [11]. Basically, we consider two distinct phases: a surface-affected liquid phase of spin-lattice relaxation rate, $1/T_{1\mathrm{surf}}$, and a bulk liquid phase of spin-lattice relaxation rate, $1/T_{1b}$, and suppose that the exchange time between them, τ_{ex}, is much smaller than both relaxation times $T_{1\mathrm{surf}}$ and T_{1b}. According to this biphasic fast exchange model, the overall proton spin-lattice relaxation rate $1/T_1(\omega_I)$ is

$$\frac{1}{T_1(\omega_I)}=\frac{1}{T_{1b}}+\frac{N_S}{N}\frac{1}{T_{1\mathrm{surf}}(\omega_I)+\tau_{\mathrm{ex}}}\approx\frac{1}{T_{1b}}+\frac{N_S}{N}\frac{1}{T_{1\mathrm{surf}}(\omega_I)}. \tag{1}$$

We demonstrated that this biphasic fast exchange model has been successful in the analysis of nuclear relaxation of polar liquids in calibrated nanopores [12]. In Eq. (1), N_S/N represents the ratio of the number of water molecules at the pore surface to the total number in the sample. From the sample characteristics listed in Table I, we show in Table II how we have estimated the ratio $N_S/N=0.054$ for $S1$ and $N_S/N=0.020$ for $S2$. The samples studied were a packed suspension of glass beads in essentially the form used for chromatographic separations. The water may be located in both the glass pores and between the glass beads. Though the latter is

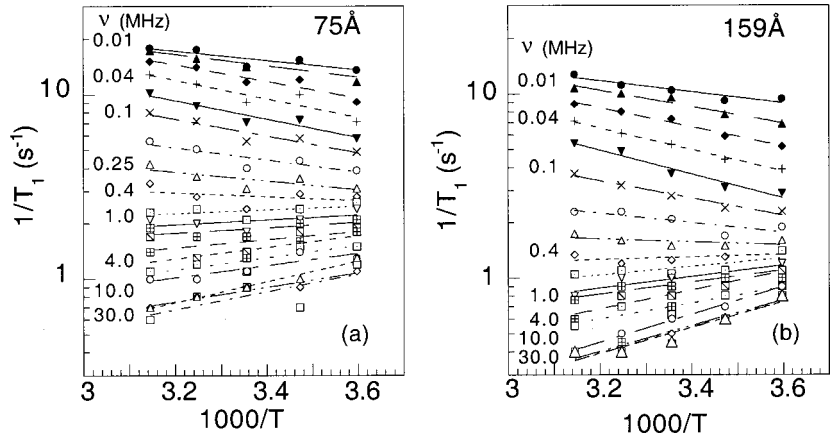

FIG. 2. Arrhenius plots of the water ^{1}H spin-lattice relaxation rates as a function of the inverse of the temperature, $1000/T$, for packed samples of calibrated porous glass beads with pore diameters 75 Å (a) and 159 Å (b) at various frequencies varying from 0.01 to 30 MHz downwards. The continuous lines correspond to the best exponential fits. According to Eq. (18), the slopes of these fits give, at low magnetic fields, the apparent activation energy (E_m-E_a') for the proton mobility in the surface layer.

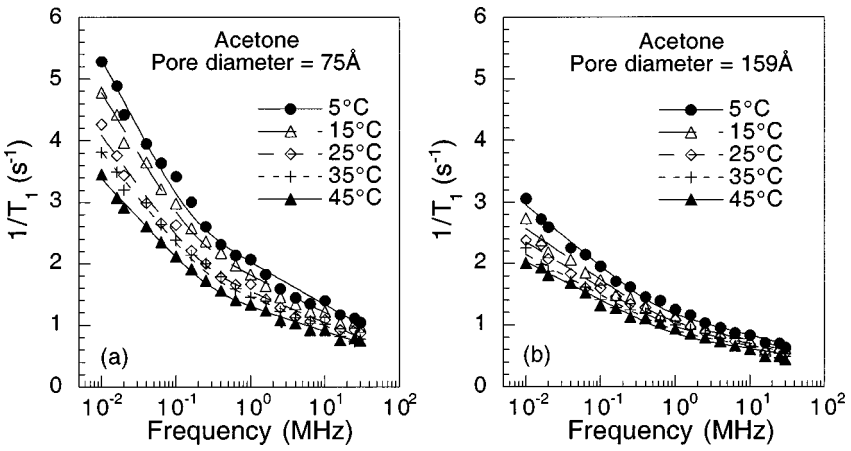

FIG. 3. The acetone ^{1}H spin-lattice relaxation rates as a function of magnetic field strength represented as the Larmor frequency for packed samples of calibrated porous glass beads with pore diameters 75 Å (a) and 159 Å (b) at various temperatures. The continuous lines correspond to the best fits to Eq. (19) of Ref. [4].

bulk water that might not mix by diffusion into and out of the beads, we have observed a single exponential decay in the time of the relaxation measurement. The relaxation rate in the bulk or nonsurface phase, $1/T_{1b}$, is caused by the fast molecular reorientations and translations and independent of magnetic field strength or frequency in the low field range studied [5]. A formal expression of $1/T_{1\mathrm{surf}}$ is obtained by mixing the relaxation of the water protons in the first coordination sphere of Fe^{3+} with the protons at surface:

$$\frac{1}{T_{1\mathrm{surf}}(\omega_I)}=\frac{1}{T_{1s}(\omega_I)}+\frac{N_{\mathrm{Fe}}}{N_S}\frac{1}{T_{1\mathrm{Fe}}+\tau_m(T)}. \qquad (2)$$

Here we have divided the proton spins belonging to the surface layer in two groups: those of nuclear relaxation rate $1/T_{1\mathrm{Fe}}$, belonging to the first coordination sphere of the paramagnetic centers and those of rate $1/T_{1s}(\omega_I)$, diffusing on the surface around such centers. The temperature-dependent exchange lifetime $\tau_m(T)$ of water between Fe^{3+} first coordination sphere and the surface phase water is given by $\tau_m=(h/kT)\exp[\Delta H^{\ddagger}/R_bT-\Delta S^{\ddagger}/R_b]$, where $\Delta H^{\ddagger}$ and $\Delta S^{\ddagger}$ are the enthalpy and entropy of activation for the first-order rate constant for the exchange for water from the cation and $R_b=2$ cal/mol/K is the molar gas constant. The detailed structure of the iron sites in the glass are unknown, but we may approximate the water exchange kinetics using a hexaaquoiron(III) ion as a model for which $\Delta H^{\ddagger}=7.4$ kcal/mol and $\Delta S^{\ddagger}=-5.6$ cal/mol/K, giving $\tau_m=(8\times10^{-10}/T)\exp[7.4\,(\mathrm{kcal/mol})/R_bT]$ leading to $\tau_m\sim0.67\ \mu$s at 298 K [7]. N_{Fe}/N_S is the ratio of the number of water molecules at the surface relaxing sites to that at the pore surface. Assuming a single water molecule per iron site, we show in Table II that $N_{\mathrm{Fe}}/N=1.70\times10^{-6}$ for $S1$ and 0.52×10^{-6} for $S2$. These values are similar to those reported by Kleinberg, Kenyon, and Mitra in rocks [13]. The rate, $1/T_{1\mathrm{Fe}}=\frac{4}{3}(\gamma_I\gamma_S\hbar)^2r_{IS}^{-6}S(S+1)T_{1e}$, is determined by modulations of the electron-nuclear dipole-dipole coupling caused by fluctuations of the electron spin of the metallic center characterized by the electronic relaxation time T_{1e} [14], which is frequency-independent in the low field range studied. Taking $r_{IS}=2.7$ Å, with $S=\frac{5}{2}$ and $T_{1e}\sim4.5\times10^{-11}$ s for Fe, one finds $T_{1\mathrm{Fe}}=3\ \mu$s. Substitution of Eq. (2) into Eq. (1) yields

$$\frac{1}{T_1(\omega_I)}=\left[\frac{1}{T_{1b}}+\frac{N_{\mathrm{Fe}}}{N}\frac{1}{T_{1\mathrm{Fe}}+\tau_m(T)}\right]+\frac{N_S}{N}\frac{1}{T_{1s}(\omega_I)}, \qquad (3)$$

where the field dependence is contained in $T_{1s}(\omega_I)$ in this range of magnetic field strengths studied. Substituting the values of N_{Fe}/N, $T_{1\mathrm{Fe}}$, and $\tau_m(T)$ given above into Eq. (3), we find that the frequency-independent term in square brackets is of the order of 0.2 to 1 s^{-1}. This range is consistent with the asymptotic limits observed in Figs. 1(a) and 1(b) at large fields for each temperature. The observed magnetic field dependence of the proton relaxation rate at low fields and the large magnitude of the relaxation rate (20 s^{-1}) thus derives only from the surface diffusion term. This term is isolated by the following subtraction:

TABLE II. Parameters derived from porous glass characteristics.

Parameters	Sample $S1$	Sample $S2$
σ_S (Fe/cm^2)	5.5×10^{10}	5.1×10^{10}
$\langle d_{\mathrm{Fe\text{-}H}}\rangle$ (Å)	5.3[a]	5.7[a]
Effective pore volume: $V=V_pm_g$ (cm^3)	0.315	0.35
Effective pore surface: $S=S_pm_g$ (m^2)	93.8	39.1
Volume of the surface layer: $S\langle d_{\mathrm{Fe\text{-}H}}\rangle$ (cm^3)	0.05	0.022
$N_s/N=S\langle d_{\mathrm{Fe\text{-}H}}\rangle/(m_w/\rho_{\mathrm{water}})$ (dimensionless)	0.054	0.020
$N_{\mathrm{Fe}}/N=S\sigma_S/(m_wN_{\mathrm{Avogadro}}/18)$ (dimensionless)	1.68×10^{-6} [b]	0.52×10^{-6} [b]

[a]Average distance between a surface proton and a ferric atom in the glass, assuming a homogeneous distribution of Fe atom in the glass.

[b]Assuming a single water molecule per iron site at the pore surface.

$$\frac{N_S}{N}\frac{1}{T_{1s}(\omega_I)_{\exp}}=\frac{1}{T_1(\omega_I)_{\exp}}-\left[\frac{1}{T_{1b}}+\frac{N_{\mathrm{Fe}}}{N}\frac{1}{T_{1\mathrm{Fe}}+\tau_m(T)}\right]_{\mathrm{asymp}}. \tag{4}$$

B. Heteronuclear dipolar surface relaxation in a model porous system

1. Model

The observed dependence of the water proton spin-lattice relaxation rate on the magnetic field strength is a power law, while that for several organic solvents that are somewhat larger and without labile protons that may exchange chemically with other molecules or surface sites is bilogarithmic on the same microporous glass preparations. Water is unique among solvents in that it is small, forms extensive hydrogen bond networks, may exchange protons rapidly, binds to metal ions, and may be orientationally ordered by hydrogen bonding at a variety of surfaces [15,16]. We seek a model that distinguishes water from the other liquids, accounts for the apparent one-dimensional diffusion process that leads to the field dependence observed, and also accounts for the unusual temperature dependence.

The temperature dependence is unusual in that at low magnetic field strengths, the spin-lattice relaxation rates increase with increasing temperature [Fig. 2(a)], which is generally indicative of a thermally activated chemical exchange process. At higher magnetic field strengths, the spin-lattice relaxation rates decrease with increasing temperature [Fig. 2(a)], which is consistent with a diffusive process dominating relaxation. Further, the apparent activation parameters for the relaxation rates measured at low magnetic fields are small, smaller than generally observed for chemical exchange events.

The first coordination sphere interactions of iron with water are well studied in other contexts. The water proton exchange rate may often limit the effectiveness or the iron (III) ion paramagnetic contribution to the total proton spin-lattice relaxation rate [6,7]. We do not know exactly the nature of the surface iron sites, but may use the hexaaquoiron(III) ion as a model for these sites. The hexaaquoiron(III) ion has a mean residence time for the coordinated water proton of 0.7 μs, which is orders of magnitude longer than correlation times for diffusive motion. This lifetime is temperature dependent, and decreases with increasing temperature. In the case where the first term of Eq. (3) was dominant, this slow first-coordination sphere exchange could limit the effective spin relaxation rate and account for the increase in the relaxation rate with increasing temperature. However, dominance of the first term in Eq. (3) should produce a low field relaxation dispersion profile that is independent of magnetic field strength, which is not observed. Further the relaxation at low magnetic field strengths is too efficient to be dominated by this contribution alone. Thus, while the magnetic relaxation is clearly involved with paramagnetic effects, first-coordination sphere exchange of water protons with the iron atom fails to account for both the temperature and magnetic field dependence observed.

Effectively one-dimensional motion may result when diffusion is fast enough that a molecule may explore a significant longitudinal extent of the pore. If one conceives of a surface mobility that is substantially reduced, for which there is little evidence, a model of surface diffusion facilitated by exchange to a rapidly diffusing bulk phase may account for many aspects of the present data. However, this type of model does not correctly account for the temperature dependence at all magnetic fields studied. On the other hand, the intimate interaction of water with the surface may have several consequences: (a) The formation of extensive hydrogen bond networks is possible. (b) OH functionality at the surface may dramatically catalyze proton exchange among water molecules in the ordered surface environment. (c) Surface diffusion rates of protons may be accelerated relative to the bulk phase. These factors are, in a sense, opposite to that of the bulk-mediated diffusion picture, but naturally account for both the magnetic field and temperature dependence of the proton spin-lattice relaxation rates.

We note that other approaches may yield the power-law magnetic field dependence observed here. For example, spin diffusion to paramagnetic relaxation sinks is well known to yield relaxation proportional to the reciprocal of the square root of the Larmor frequency. Even though we suppose a surface-ordered phase, which may have many characteristics of a solid, spin diffusion should be unimportant compared with other contributions for the following reasons. (a) The presumed hydrogen surface network is imperfect so that we expect that there would be a number of spin diffusion bottlenecks that would inhibit extensive or long-range diffusion. (b) The relatively high mobility of the surface phase will reduce the correlation time that enters the effective dipole-dipole coupling between surface water spins. As a result, the spin-diffusion constant will be reduced from the usual values in rigid solids, which are already small. (c) The small surface spin-diffusion rate that results will be too small to contribute to an extensive diffusion of spin along the pore to a remote relaxation center. Thus, we conclude that spin diffusion as distinct from translational diffusion cannot account for the present data.

The Kimmich group has investigated related systems, which are reported to be free of paramagnetic impurities, and proposed a fundamentally different model involving effectively one-dimensional correlation effects based on purely nuclear spin interactions [1]. Because nuclear-spin relaxation in the present case is apparently much more efficient, and the presence of paramagnetic relaxation centers demonstrated by EPR spectroscopy and chemical analysis, we seek an alternative model.

2. Calculation of the proton surface spin-lattice relaxation rate

We consider water in an infinite cylindrical pore of radius R with a surface density σ_S of paramagnetic centers S as shown in Fig. 4(a). The water protons at the surface diffuse over a certain surface region and then suffer a chemical exchange to the bulk liquid region of the pore. The proton relaxation rates are too large to be accounted for by only nuclear dipolar couplings. Thus, the model is based on electron-nuclear dipolar couplings, which are about five orders of magnitude more effective in the nuclear spin relaxation equations [5]. The intermolecular electron-nuclear dipole-dipole coupling is modulated by the translational diffusion of the mobile I spins in close proximity to the pore

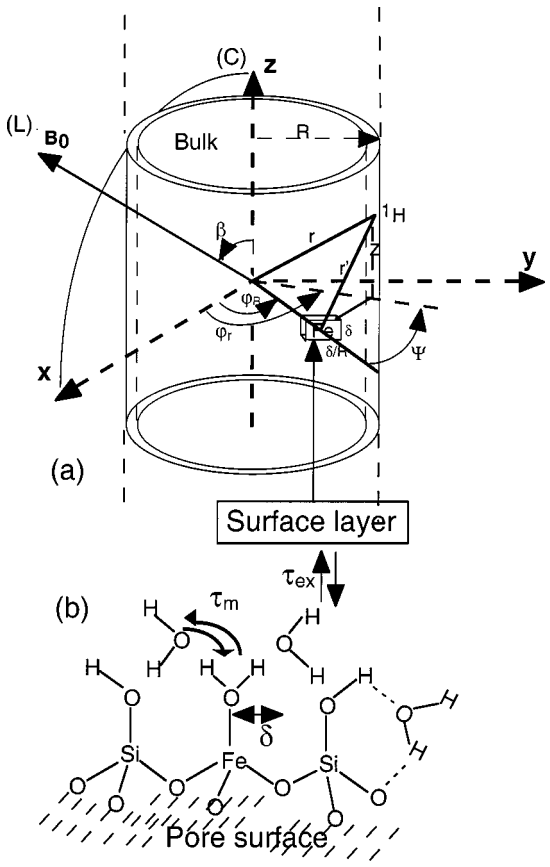

FIG. 4. (a) Schematic diagram of the cylindrical pore model. The nuclear proton spin I diffuses in the surface layer of thickness $\langle d_{\text{Fe-H}}\rangle \sim 5.3$ Å in the dipolar field of a very small quantity of paramagnetic spins S fixed on the pore surface. The (C) axes are fixed in the cylindrical frame. The (L) axes are fixed in the laboratory frame, with the constant magnetic field $\mathbf{B}_0$ at the angle β from the pore axis $\mathbf{z}$. (b) Schematic diagram of the pore surface layer in the close vicinity of the ferric ion. δ is the distance of minimal approach along z between the mobile proton and the ferric ion. The distinction between the correlation times τ_m for chemical exchange in the surface layer and, τ_{ex} between the surface and the bulk is indicated on the diagram. The dashed lines represent the hydrogen bonds.

surface and the fixed S spins. Formally, the proton spin-lattice relaxation is given by the general expression [5]:

$$\frac{1}{T_{1I}} = \frac{2}{3}(\gamma_I\gamma_S\hbar)^2 S(S+1)\left[\tfrac{1}{3}J_L^{(0)}(\omega_I-\omega_S) + J_L^{(1)}(\omega_I) + 2J_L^{(2)}(\omega_I+\omega_S)\right], \tag{5}$$

where the spectral density $J_L^{(m)}$ in the laboratory frame (L) associated with $\mathbf{B}_0$ [Fig. 4(a)] are the exponential Fourier transforms,

$$J_L^{(m)}(\omega) = \int_{-\infty}^{\infty} G_L^{(m)}(\tau) e^{i\omega\tau}\, d\tau, \tag{6a}$$

of the stationary pairwise dipolar correlation functions $G_L^{(m)}(\tau)$, $\{m \in (-2,+2)\}$, given by

$$G_L^{(m)}(\tau) = \langle F_L^{(-m)}(t) F_L^{(-m)*}(t+\tau)\rangle. \tag{6b}$$

Equation (6b) describes the persistence of the second-order irreducible spherical spatial dipolar tensor, $F_L^{(m)}(t)$, between the magnetic moments associated with the spins I and S and modulated by the translational diffusion of spins I relative to the fixed spins S during a short time interval τ [5]. The notation $\langle\,\rangle$ stands for the ensemble average over all the positions of the spins I at times 0 and τ for a given surface density σ_S of spins S. Simplification of Eq. (5) occurs when $\omega_S \gg \omega_I$. As found below, substitution of spectral densities that depend on the inverse of the square root of the Larmor frequency into Eq. (5) shows that

$$\frac{1}{T_{1I}(\omega_I)} \approx \frac{2}{3}(\gamma_I\gamma_S\hbar)^2 S(S+1) J_L^{(1)}(\omega_I). \tag{7}$$

According to the dynamical model described in Figs. 4(a) and 4(b), it is efficient to calculate the time dependencies of the dipolar correlations in the cylindrical frame (C) of $\mathbf{z}$ axis parallel to the pore axis. We use the well-known properties of the Wigner D functions [17] to express $F_L^{(1)}(t)$ as it comes through a rotation: $(C)\rightarrow(L)$,

$$F_L^{(-1)}(t) = \sqrt{\frac{6\pi}{5}} \frac{1}{r'^3(t)} \sum_{m'=-2}^{2} Y_2^{(m')}(\Omega'(t)) d_{-1,m'}^{(2)}(\beta). \tag{8}$$

Here r' represents the proton (I)-electron (S) distance at time t and $Y_2^{(m')}(\Omega'(t))$ represent the second-order spherical harmonics where the angles labeled as $\Omega'(t)$ follow the orientation of $\mathbf{r}'$ in (C). Because of cylindrical symmetry around $\mathbf{z}$ we have chosen the Euler angles that rotate the (C) frame into the (M) frame as $\alpha=\gamma=0$; thus, the general Wigner rotation matrix, $D_{-1m'}^{(2)}(\alpha=0,\beta,\gamma=0)$ reduces to the tabulated Wigner coefficients $d_{-1m'}^{(2)}(\beta)$ [17]. After substitution of Eq. (8) in $G_L^{(1)}(\tau) = \langle F_L^{(-1)}(t) F_L^{(-1)*}(t+\tau)\rangle$ and application of some symmetry relations, one has for the pairwise dipolar correlation function in the (L) frame:

$$G_L^{(-1)}(\tau) = \frac{6\pi}{5} \sum_{m'=-2}^{+2} |d_{-1,m'}^{(2)}(\beta)|^2 G_C^{(m')}(\tau), \tag{9}$$

where the components $G_C^{(m')}(\tau)$ of the pairwise dipolar correlation function in the (C) frame are

$$G_C^{(m')}(\tau) = \left\langle \frac{Y_2^{(m')}(\Omega_0')}{r_0'^3} \frac{Y_2^{(m')*}(\Omega')}{r'^3} \right\rangle. \tag{10}$$

Now we make a powder average over the angle β labeled as $\langle\,\rangle_\beta$ in order to take into account the random orientation of the local cylindrical axis $\mathbf{z}$ relative to the constant direction of the static magnetic field $\mathbf{B}_0$,

$$\langle G_L^{(-1)}(\tau)\rangle_\beta = \frac{6\pi}{5} \sum_{m'=-2}^{+2} \langle |d_{-1,m'}^{(2)}(\beta)|^2\rangle_\beta G_C^{(m')}(\tau) = \frac{1}{5}\frac{6\pi}{5} \sum_{m'=-2}^{+2} G_C^{(m')}(\tau). \tag{11}$$

When considering translational diffusion of the I spin at the surface of the geometry shown in Figs. 4(a) and 4(b), the average present in Eqs. (10) and (11) will be replaced by their usual integral average over the normalized conditional probability $P(\rho=R,\varphi_r,z,\tau|\rho_0=R,\varphi_{r0},z_0,\tau=0)$ that the protonic cylindrical coordinates $\rho=R,\varphi_r$ in (x,y) and $z(\|\mathbf{z})$ take their values at time τ, given their values $\rho_0=R,\varphi_{r0}$, z_0 at time $\tau=0$,

$$G_C^{(m')}(\tau)=\sigma_S\int_{C_\varphi}R\,d\varphi_{r0}\int_{C_z}dz_0\frac{Y_2^{(m')}(\Omega_0')}{r_0'^3}\times\int_{C_\varphi}R\,d\varphi_r\int_{C_z}dz\,P(\rho=R,\varphi_r,z,\tau|\rho_0=R,\varphi_{r0},z_0,\tau=0)\frac{Y_2^{(m')*}(\Omega')}{r'^3}. \tag{12}$$

Here we have assumed a uniform proton surface density at equilibrium and C_φ and C_z correspond to the φ_r and z domains of integration in the C frame [see Appendix and Fig. 4(a)].

Following previous proton NMR studies for different ice-silica interfaces [16], we suppose that proton diffusion at the liquid-solid interface is enhanced by orientational ordering of water molecules in the first layers [Fig. 4(b)]. The probability of a water molecule participating in the ordered phase is proportional to a Boltzmann factor, $n_0\exp(E_m/R_bT)$, where n_0 is the maximum number of molecules in the ordered domain, R_b is the molar gas constant, and E_m is unknown but expected to be larger than that for motions in bulk water, i.e., $\sim$5 kcal/mol. The effective size of the ordered domain in the surface layer will then vary in proportion to $2\delta_w n_0\exp(E_m/R_bT)$. Here $\delta_w=1.9$ Å is the effective radius of a water molecule based on the density of liquid, which implies a volume per water molecule of 30 Å^3. We may estimate the rate at which these clusters rearrange based on the properties of bulk water; thus, the rearrangement time is approximated by $\tau_w=\delta_w^2/\{D_0\exp(-E_a/R_bT)\}$, where $E_a=4.8$ kcal/mol is the activation energy for the water translational diffusion. Now, assuming that a proton suffers rapid diffusive motion inside a surface layer, which evolves on a much slower time scale τ_w, we get an effective two-dimensional diffusion equation for P as

$$\frac{\partial}{\partial\tau}P(\rho=R,\varphi_r,z,\tau|\rho_0=R,\varphi_{r0},z_0,\tau=0)=\frac{\delta_w^2}{\tau_w}n_0e^{E_m/RT}\times\Delta_S P(\rho=R,\varphi_r,z,\tau|\rho_0=R,\varphi_{r0},z_0,\tau=0). \tag{13}$$

Inspection of Eq. (13) implies that the effective diffusion constant of the surface protons in the ordered phase $D_{\rm eff}(T)=D_{\rm eff\,0}\exp[(E_m-E_a')/R_bT]$, where $D_{\rm eff\,0}=D_0'n_0$, E_a' is the activation energy for the translational motion in the surface-ordered phase. The fact that $E_m>E_a'$ leads to a diminution of the effective diffusion coefficient $D_{\rm eff}(T)$, with increasing temperature and may account for the low field temperature dependence of the proton spin-lattice relaxation rate.

At times longer than that required to diffuse a pore radius, approximately $\tau_R=R^2/(2D_w)\sim3.5\times10^{-9}$ s, where $D_w\sim2.2\times10^{-5}$ cm^2/s is the bulk water translational diffusion, P becomes independent of any orientational angular random variables φ_r and depends only on the cylindrical coordinate z along the pore axis. In this case, diffusion that affects nuclear spin relaxation has a one-dimensional character and is driven by diffusion along the pore axis. In the model that we used here, P represents the probability of reencounters per unit area between I and S spins; it is given by the Gaussian propagator:

$$P(z,\tau|z_0=0,\tau=0)=\frac{1}{2\pi R}\frac{1}{(4\pi D_{\rm eff}\tau)^{1/2}}\exp\left(-\frac{z^2}{4D_{\rm eff}\tau}\right). \tag{14}$$

Successive substitutions of Eq. (14) into Eqs. (11) and (12) lead to the following simplification:

$$\langle G_L^{(-1)}(\tau)\rangle_\beta=\frac{1}{5}\frac{6\pi}{5}[G_C^{(0)}(\tau)+2G_C^{(1)}(\tau)+2G_C^{(2)}(\tau)]\approx\frac{1}{5}\frac{6\pi}{5}G_C^{(0)}(\tau). \tag{15}$$

After calculations of Eq. (15) detailed in Appendix A, one finds that at long times ($\tau\gg\tau_R$), the dominant term of the pairwise dipolar correlation function is given by the power law

$$\langle G_L^{(-1)}(\tau)\rangle_\beta=\frac{3}{10\pi}\frac{\sigma_S}{R\delta^2}\frac{1}{(4\pi D_{\rm eff}\tau)^{1/2}}, \tag{16}$$

where δ corresponds to the distance, along z, of minimal approach of a proton to a Fe^{3+} ion. From the model presented in Fig. 4(b), we chose $\delta\sim0.85$ Å, which corresponds to the known minimal distance $r_{IS}=2.7$ Å, between the proton and ferric ion. The corresponding averaged spectral density thus becomes

$$J_L^{(1)}(\omega)=\frac{3\sqrt{2}}{20\pi}\frac{\sigma_S}{R\delta^2}\frac{1}{(D_{\rm eff}\omega)^{1/2}}. \tag{17}$$

After substitution of Eq. (17) into Eq. (7) and multiplication by the dilution factor (N_S/N), one has finally the following theoretical expression for the surface proton spin-lattice relaxation rate, at low field strengths, for the model considered:

$$\frac{N_S}{N}\frac{1}{T_{1s}(\omega_I)}=\frac{\sqrt{2}}{10\pi}\frac{N_S}{N}(\gamma_I\gamma_S\hbar)^2S(S+1)\frac{\sigma_S}{R\delta^2}\times\frac{1}{(D_{\rm eff}(T)\omega_I)^{1/2}}. \tag{18}$$

A consequence of Eq. (18) is that the apparent activation energy for the low-field relaxation rate is $-(E_m-E_a')/2$ because the exponent of $D_{\rm eff}(T)$ is (E_m-E_a'). This result further reduces the magnitude of the apparent activation energy for the low-field relaxation processes. From the Arrhenius plots of Fig. 2, one finds that this apparent activation energy (E_m-E_a') is 2.4 kcal/mol for $S1$ and 2.8 kcal/mol for $S2$ at low fields (0.01 MHz). Taking an average value for $(E_m-E_a')=2.6$ kcal/mol and assuming that $E_a'\sim E_a=4.8$ kcal/mol, one has an estimation of $E_m\sim 7.4$ kcal/mol for the activation energy, for the proton mobility in the surface layer.

IV. COMPARISON WITH EXPERIMENTS

A. Magnetic relaxation dispersion of water in confinement

The best fits obtained with Eqs. (3) and (18) for $1/T_1(\omega_I)_{\rm exp}$ and with Eq. (18) for $(N_S/N)1/T_{1s}(\omega_I)_{\rm exp}$ are shown as continuous lines, in Figs. 1(a) and 1(c) for $S1$ and in Figs. 1(b) and 1(d) for $S2$. These lines were obtained with the apparent activation energy, $(E_m-E_a')=2.6$ kcal/mol, for the proton mobility in the surface layer. All the other parameters present in Eq. (18) are given in Table II. The only adjustable parameter is the prefactor $D_{\rm eff\,0}$. For $S1$, we find $D_{\rm eff\,0}=0.106\times10^{-6}$ cm^2/s giving $D_{\rm eff}=0.85\times10^{-5}$ cm^2/s at 25 °C. This value, for the proton surface diffusion of the order of one third of the bulk water translational diffusion $D_w\sim 2.2\times10^{-5}$ cm^2/s, is in very good agreement with recent neutron-scattering studies of single-particle dynamics of water molecules contained in 25% hydrated micropores of vycor glass [18]. This value is also in agreement with molecular-dynamics simulation of liquid water on silica surfaces [19]. Similarly for the large pore glass ($S2$), one finds $D_{\rm eff\,0}=0.03\times10^{-6}$cm^2/s and $D_{\rm eff}=0.24\times10^{-5}$cm^2/s at 25 °C. The diminution of the $D_{\rm eff}$ value found for $S2$ in comparison with the one for $S1$ is coherent with the diminution of the effective pore surface and of N_S/N (Table II). This result is also in good agreement with water surface diffusion measurements on silica gels [20]. According to Eq. (18), the pore size effect ($\propto 1/R$) is smaller than the one ($\propto 1/R^2$) obtained previously for an aprotic solvent [4]. This is coherent with the results shown in Figs. 1 and 3.

The seemingly paradoxical increase of the water proton spin-lattice relaxation rate observed at low fields when the temperature increases [Figs. 2(a) and 2(b)] is understood in terms of a diminution of the effective spatial extension of the quasiordered clusters of water molecules in the surface layer close to the paramagnetic impurity. The chemical exchange process ($\tau_{\rm ex}$) between the surface layer and the bulk [Fig. 4(b)] interrupts the proton surface diffusion and limits the extent of the surface-enhanced diffusion. When the temperature increases, the extent of the ordered domains decreases and surface mobility is reduced, thus causing the low-field relaxation rate to increase. The confinement results in an enhancement of the probability of I-S reencounters, which maintain the dipolar correlations for a much longer time.

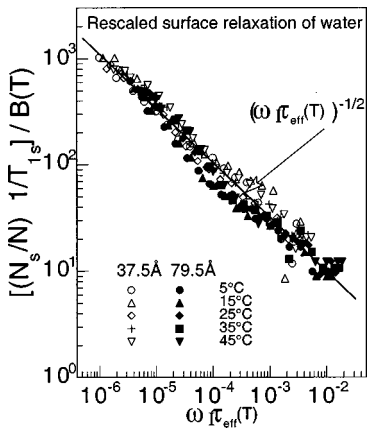

FIG. 5. Logarithmic plot of the rescaled magnetic field dependence of the dimensionless surface ^{1}H spin-lattice relaxation rates, $(N_S/N)1/T_{1s}(\omega_I)/B(T)$ of water in packed samples of calibrated porous glass beads of pore radii 37.5 and 79.5 Å at various temperatures as a function of the dimensionless variable $\omega_I\tau_{\rm eff}(T)$ with $\tau_{\rm eff}(T)=\tau_{\rm eff\,0}\exp[-(E_m-E_a)/R_bT]$. The data points are obtained by rescaling those of Figs. 1(c) and 1(d) according to Eqs. (19a) and (19b). The continuous line is the best fit obtained with the relation $1/[\omega_I\tau_{\rm eff}(T)]^{1/2}$.

An estimate of the distance explored by the proton before the first reencounter with the ferric ion on the surface is of the order of the length of diffusion, $[2D_{\rm eff}/\nu_c]^{1/2}$, where ν_c is a characteristic frequency, shown by an arrow in Fig. 1(a). Below ν_c the relaxation rate increases rapidly and the temperature dependence becomes abnormal. With $D_{\rm eff}=0.85\times10^{-5}$ cm^2/s at 25 °C and $\nu_c\sim 3$ MHz [Fig. 1(a)], one finds that this distance is about 238 Å for $S1$ and 126 Å for $S2$. Such distances of exploration are sufficiently large in comparison to the pore radius R to make the dynamics appear one-dimensional and justify the model proposed.

An important consequence of the proposed model is found by introducing into Eq. (18), the effective correlation time of surface diffusion, $\tau_{\rm eff}(T)=\delta_w^2/[2D_{\rm eff}(T)]$, which gives the following universal power law:

$$\frac{N_S}{N}\frac{1}{T_{1s}(\omega_I)}\frac{1}{B(T)}=\frac{1}{\sqrt{\omega_I\tau_{\rm eff}(T)}}, \tag{19a}$$

with

$$B(T)=\frac{1}{5\pi}\frac{N_S}{N}(\gamma_I\gamma_S\hbar)^2S(S+1)\frac{\sigma_S}{R\delta^2\delta_w}\tau_{\rm eff}(T). \tag{19b}$$

In Fig. 5, we show that the experimental values of the surface dispersion $(N_S/N)1/T_{1s}(\omega_I)_{\rm exp}$ displayed in Figs. 1(c) and 1(d) could be rescaled as $[\omega_I\tau_{\rm eff}(T)]^{-1/2}$ over four orders of magnitude of the dimensionless variable $\omega_I\tau_{\rm eff}(T)$.

This power law is usually encountered in the presence of a one-dimensional translational diffusion relaxation process [21]. To calculate the effective correlation time for each temperature, $\tau_{\rm eff}(T)=\tau_{\rm eff\,0}\exp[-(E_m-E_a')/R_bT]$, we use the relation, $\tau_{\rm eff\,0}=\delta_w^2/(2D_{\rm eff\,0})$, and the values of $D_{\rm eff\,0}$ found above. This approach gives $\tau_{\rm eff\,0}=1.7\times10^{-9}$ s and $\tau_{\rm eff}(25\,^\circ{\rm C})=2.1\times10^{-11}$ s for $S1$ and $\tau_{\rm eff\,0}=6.0\times10^{-9}$ s and $\tau_{\rm eff}(25\,^\circ{\rm C})=7.5\times10^{-11}$ s for $S2$. This universal rescaling obtained for 200 experiments on different samples ($S1$ and $S2$) and on a large variety of frequencies and temperatures, strongly supports the model used here.

B. Magnetic relaxation dispersion of aprotic solvent (acetone) in confinement

The situation is very different for acetone, which has no exchangeable protons. Acetone is a poor Lewis base compared with water, and is a poor ligand for the iron atom. Although one could argue that there will be some equilibrium for binding of the acetone oxygen to the iron, the equilibrium will favor water by many orders of magnitude. Further, we do not see specific evidence that acetone binds. If it did, the contribution would be much smaller than it would be for the water because the protons would be much further away from the metal center than in the water case. Thus, the contribution to the spin relaxation from first coordination effects should be much smaller than in the water case. In consequence it is an excellent approximation that the acetone does not bind significantly to the iron. The observed bilogarithmic magnetic field dependence of proton $1/T_{1s}$, displayed in Figs. 3(a) and 3(b), is consistent with a theory that treats the mobile liquid spins from the viewpoint of two-dimensional restricted diffusion at a proximity of a relaxing surface center [4]. In this case, a two-dimensional translational diffusion in close proximity to the relaxing sites is needed and the slower diffusion associated ($D\sim0.14\times10^{-5}$ cm^2/s) precludes exploration of the distant relaxation sites in the pore.

V. CONCLUSION

^{1}H MRD experiments of water in contact with microporous glass surfaces containing trace paramagnetic impurities is fundamentally different from that found for aprotic solvents. In all cases the nuclear-spin relaxation rates at low magnetic field strengths are dominated by contributions from trace paramagnetic impurities in the solid matrix. The effects of the liquid confinement is that long-time correlations are introduced that increase the reencounter probability at long times or low Larmor frequencies. The comparison between water and acetone shows that the apparent dimensionality of the diffusive process is a function of the surface mobility and the effective concentration of the paramagnetic relaxation centers. For the organic solvents studied, the spatial extent explored by the diffusing solvent is relatively small and relaxation is described by a two-dimensional diffusive process that causes a bilogarithmic dependence of the relaxation rate on the Larmor frequency. For water we find that the effective proton diffusion rate at the surface is facilitated. We have developed a general model of nuclear-spin relaxation caused by a surface-facilitated proton diffusive process. This model naturally leads to a relaxation equation characteristic of a one-dimensional diffusive process and also accounts for the peculiar temperature dependence of the water-proton relaxation rates at different magnetic field strengths. A universal rescaling obtained for these data on different pore sizes and on a large variety of magnetic field strengths and temperatures, supports this interpretation. The unique frequency and temperature dependencies of the proton MRD have allowed a direct assessment of the translational diffusion coefficient of water protons at the surface of the pores. The model employed is fundamentally different from previous approaches to similar problems, but appears to have a number of features that will be generally applicable in a number of contexts.

ACKNOWLEDGMENTS

The authors gratefully acknowledge useful discussions with Dr. P. Levitz and Dr. D. Petit, and support by the National Institutes of Health (USA) GM-39309, GM34541 and the University of Virginia.

APPENDIX: CALCULATION OF CORRELATION FUNCTIONS $G_C^{(0)}(\tau)$, and $\langle G_L^{(1)}(\tau)\rangle_\beta$

The surface pairwise dipolar correlation function, $G_C^{(0)}(\tau)$, remaining at long times in the cylindrical frame C, is given from Eqs. (12) and (14):

$$G_C^{(0)}(\tau)=\frac{\sigma_S}{2\pi R}\frac{1}{(4\pi D_{\rm eff}\tau)^{1/2}}\times\int_{C_\varphi}R\,d\varphi_{r0}\int_{C_z}dz_0\frac{Y_2^{(0)*}(\Omega_0')}{r_0'^3}\int_{C_\varphi}R\,d\varphi_r\int_{C_z}dz\times\exp\left(-\frac{z^2}{4D_{\rm eff}\tau}\right)\frac{Y_2^{(0)*}(\Omega')}{r'^3}. \tag{A1}$$

Due to the relation $\mathbf{r}'=\mathbf{r}-\mathbf{R}$ and the restriction $r=(R^2+z^2)^{1/2}$, where the proton moves at the cylindrical pore surface [Fig. 4(b)], one can express the spherical harmonics in the cylindrical frame C as

$$\frac{Y_2^0(\Omega')}{r'^3}=\frac{1}{4}\sqrt{\frac{5}{\pi}}\left\{\frac{3z^2}{\left[z^2+4R^2\sin^2\left(\frac{\varphi_r-\varphi_R}{2}\right)\right]^{5/2}}-\frac{1}{\left[z^2+4R^2\sin^2\left(\frac{\varphi_r-\varphi_R}{2}\right)\right]^{3/2}}\right\}. \tag{A2}$$

Expression of $G_C^{(0)}(\tau)$ simplifies after substitution of Eq. (A2) in Eq. (A1) and using the reasonable assumption that, at long times, the diffusion length $\sqrt{(2D_{\rm eff}\tau)}\sim0.4\,\mu$m stays much larger than any possible z values ($\sim$250 Å),

$$G_C^{(0)}(\tau)=\frac{5\sigma_S}{32\pi^2 R}\frac{1}{(4\pi D_{\rm eff}\tau)^{1/2}}\left|\int_{C_\varphi}Rd\varphi_r\int_{C_z}dz\right.$$
$$\times\left\{\frac{3z^2}{\left[z^2+4R^2\sin^2\left(\frac{\varphi_r-\varphi_R}{2}\right)\right]^{5/2}}\right.$$
$$\left.\left.-\frac{1}{\left[z^2+4R^2\sin^2\left(\frac{\varphi_r-\varphi_R}{2}\right)\right]^{3/2}}\right\}\right|^2. \quad \text{(A3)}$$

The integration in z in Eq. (A3) in the domain C_{z1} where $|z|>\delta$ is elementary. Here δ corresponds to the distance, along z, of minimal approach between a proton and a Fe^{3+} ion. From the model presented in Fig. 4(b), we choose $\delta\sim 0.85$ Å, which corresponds to the known minimal distance $r_{IS}=2.7$ Å, between the proton and ferric ion.

$$\int_{C_{z1}}dz\left\{\frac{3z^2}{\left[z^2+4R^2\sin^2\left(\frac{\varphi_r-\varphi_R}{2}\right)\right]^{5/2}}\right.$$
$$\left.-\frac{1}{\left[z^2+4R^2\sin^2\left(\frac{\varphi_r-\varphi_R}{2}\right)\right]^{3/2}}\right\}$$
$$=\frac{2}{\delta^2\left[1+4\frac{R^2}{\delta^2}\sin^2\left(\frac{\varphi_r-\varphi_R}{2}\right)\right]^{3/2}}. \quad \text{(A4)}$$

A similar result but with an opposite sign is found in the domain C_{z2} where $-\delta\leqslant z\leqslant\delta$. Introducing the variable $\psi=\varphi_r-\varphi_R$ and taking into account the even character of the function on the integration on ψ, one finds that there are two domains for C_ψ. The first domain, $C_{\psi 1}=(0\leqslant\psi\leqslant\pi)$, of complete cylindrical isotropy is associated with C_{z1}. The second domain, $C_{\psi 2}=(\delta/R\leqslant\psi\leqslant\pi)$, is associated with C_{z2} and excludes a small domain in the immediate surrounding of the Fe^{3+} ion. Straightforward calculations show that the only remaining integral on ψ becomes

$$\frac{4R}{\delta^2}\int_0^{\delta/R}d\Psi\left[1+4\frac{R^2}{\delta^2}\sin^2\left(\frac{\Psi}{2}\right)\right]^{-3/2}$$
$$\approx\frac{4R}{\delta^2}\left(\frac{1}{\sqrt{2}}\frac{\delta}{R}+O\left(\frac{\delta^2}{R^2}\right)\right)\approx\frac{2\sqrt{2}}{\delta}. \quad \text{(A5)}$$

Substituting Eq. (A5) into Eq. (A3) leads to the form

$$G_C^{(0)}(\tau)=\frac{5\sigma_S}{4\pi^2 R\delta^2}\frac{1}{(4\pi D_{\rm eff}\tau)^{1/2}}. \quad \text{(A6)}$$

Finally, substitution of Eq. (A6) into Eq. (15) leads to the surface pairwise dipolar correlation function, $\langle G_L^{(1)}(\tau)\rangle_\beta$, remaining at long times in the laboratory frame L:

$$\langle G_L^{(1)}(\tau)\rangle_\beta=\frac{3}{10\pi}\frac{\sigma_S}{R\delta^2}\frac{1}{(4\pi D_{\rm eff}\tau)^{1/2}}. \quad \text{(A7)}$$

[1] R. Kimmich and H. W. Weber, Phys. Rev. B **47**, 11 788 (1993); S. Stapf and R. Kimmich, J. Chem. Phys. **103**, 2247 (1995).
[2] S. Stapf, R. Kimmich, and R. O. Seitter, Phys. Rev. Lett. **75**, 2855 (1995).
[3] M. Whaley-Hodges, A. J. Lawrence, J.-P. Korb, and R. G. Bryant, Solid State Nucl. Magn. Reson. **7**, 247 (1996).
[4] J.-P. Korb, M. Whaley-Hodges, and R. G. Bryant, Phys. Rev. E **56**, 1934 (1997).
[5] A. Abragam, *The Principles of Nuclear Magnetism* (Clarendon, Oxford, 1961).
[6] I. Bertini, F. Capozzi, C. Luchinat, and Z. Xia, J. Phys. Chem. **97**, 1134 (1993).
[7] S. K. Sur and R. G. Bryant, J. Phys. Chem. **99**, 6301 (1995).
[8] A. G. Redfield, W. Fite, and H. E. Bleich, Rev. Sci. Instrum. **39**, 710 (1968).
[9] S. H. Koenig and W. E. Schillinger, J. Biol. Chem. **12**, 3283 (1969).
[10] G. Hernandez, M. F. Tweedle, H. Brittain, and R. G. Bryant, Inorg. Chem. **29**, 985 (1990).
[11] J. Korringa, D. O. Seevers, and H. C. Torrey, Phys. Rev. **127**, 1143 (1962).
[12] J.-P. Korb, L. Malier, F. Cros, Shu Xu, and J. Jonas, Phys. Rev. Lett. **77**, 2312 (1996).
[13] R. L. Kleinberg, W. E. Kenyon, and P. P. Mitra, J. Magn. Reson., Ser. A **108**, 206 (1994).
[14] I. Solomon, Phys. Rev. **99**, 559 (1955); N. Bloembergen and L. O. Morgan, J. Chem. Phys. **34**, 842 (1961).
[15] A. G. Pelmenschokov, G. Morosi, and A. Gamba, Nuovo Cimento A **19**, 1749 (1997).
[16] J. Ocampo and J. Kilinger, J. Phys. Chem. **87**, 4325 (1983).
[17] D. A. Varshalovich, A. N. Moskalev, and V. K. Khersonskii, *Quantum Theory of Angular Momentum* (World Scientific, Singapore, 1988), Chap. 4.
[18] M. C. Bellissent-Funel, S. H. Chen, and J. M. Zanotti, Phys. Rev. E **51**, 4558 (1994).
[19] S. H. Lee and P. J. Rossky, J. Chem. Phys. **100**, 3334 (1994).
[20] C. F. Polnazek, D. Hanggi, P. W. Carr, and R. G. Bryant, Anal. Chim. Acta **194**, 311 (1987).
[21] M. Villa, L. Borghi, A. De Ambrosis, and S. Aldrovandi, Nuovo Cimento A **2**, 1019 (1983).